Journal of Building Engineering 101 (2025) 111834

Contents lists available at ScienceDirect

Journal of Building Engineering

journal homepage: www.elsevier.com/locate/jobe

Seismic vulnerability assessment of historical buildings in Sofia: A multi-Methodological approach

Gaetano Pianese [a], Nicola Chieffo [b], Gabriele Milani [a], Doncho Partov [c], Antonio Formisano [d,*]

[a] Department of Architecture, Built Environment and Construction Engineering, Politecnico di Milano P.za Leonardo da Vinci, 32, Milan, Italy
[b] Department of Engineering School of Computing and Engineering, University of Huddersfield, Queensgate Huddersfield, HD1 3DH, United Kingdom
[c] University of Structural Engineering & Architecture "Lyuben Karavelov" ul. "Suhodolska" 175, 1373, Sofia, Sofia, Bulgaria
[d] Department of Structures for Engineering and Architecture, School of Polytechnic and Basic Sciences, University of Naples Federico II, Naples, Italy

A R T I C L E I N F O

Keywords:
Seismic vulnerability assessment
Typological vulnerability curves
Urban seismic risk scenario
Historical buildings
Sofia (Bulgaria)

A B S T R A C T

The proposed research aims to estimate the seismic vulnerability of historical buildings in a district of Sofia, Bulgaria. Initially, a sample of buildings was selected, and an inventory was created based on their structural and typological characteristic using the Italian CARTIS form and the EMS-98 scale. Following this, a comprehensive vulnerability assessment of the built environment was conducted using a multi-level analysis. This involved the application and comparison of three methodologies, including RISK-UE, a vulnerability index-based approach tailored for clustered buildings, and the procedure SAVE (Strumenti Aggiornati per la Vulnerabilità sismica del patrimonio Edilizio e dei sistemi urbani – Updated Tools for the Seismic Vulnerability Evaluation of the Italian Real Estate and of Urban Systems). The findings were incorporated into a Geographic Information System (GIS) tool to visualize the distribution of seismic vulnerability across the studied urban area. Additionally, a parametric analysis was performed to explore various potential damage scenarios. This analysis utilized an intensity prediction equation derived from Sofia's historical earthquake records, considering different values for macroseismic intensity, moment magnitude, and epicenter distance to provide a comprehensive overview of the assets at risk.

1. Introduction

Recent global earthquakes have underscored the poor seismic performance of buildings, particularly historical ones. It is well known that older structures were constructed without specific seismic design criteria. In these cases, vertical structures were designed to bear only gravitational loads, providing minimal resistance to seismic horizontal forces [1,2]. These factors, combined with the physical deterioration of materials, result in significant structural vulnerability that adversely affects the overall behavior of buildings. In historical centers, the combination of high population density and poor structural conditions poses a major challenge for seismic engineering.

To mitigate seismic risk in urban areas, a comprehensive large-scale vulnerability analysis is essential [3,4]. Various methods have been developed for seismic vulnerability assessment [5–11], but their suitability can vary based on regional construction practices,

* Corresponding author.
E-mail address: antonio.formisano@unina.it (A. Formisano).

https://doi.org/10.1016/j.jobe.2025.111834
Received 14 July 2024; Received in revised form 10 January 2025; Accepted 12 January 2025
Available online 18 January 2025

building typologies, and data availability. One of the most well-known methods in the literature is the one developed by Benedetti and Petrini [7], along with the Gruppo Nazionale Difesa Terremoti (GNDT) (Italian: National Group for Earthquake Protection) approach [12]. These simplified techniques consist of assigning a score to different geometrical and structural factors to calculate a vulnerability indicator for isolated buildings. Formisano et al. [13] adopted a new vulnerability form in which it is possible to consider the mutual interaction between the aggregates. Zuccaro et al. [8] proposed a new methodology after studying damage databases available from previous seismic events in Italy. This methodology is based on the Synthetic Damage Parameter (*SDP*), where the damage condition is identified for a specific class of buildings diversified structurally and typologically. The RISK-UE methodology [11] introduced an innovative approach for creating earthquake risk scenarios applicable to various European cities. This approach operates on the premise that certain categories of buildings that have similar structural and loading characteristics are likely to sustain comparable damage during earthquakes. Consequently, a set of standardized vulnerability functions can be established for these specific building classes. In recent years, all these methodologies have been described and validated as useful tools for large-scale seismic vulnerability assessment [9,10,14–19]. The peculiarity of these methodologies is the possibility of combining them with the macroseismic method for assessing damage scenarios. The macroseismic methodology allows for evaluating the susceptibility to damage of a stock of buildings, varying the expected hazard level, defined as macroseismic intensity according to the EMS-98 scale.

Based on these premises, this study conducts a vulnerability assessment of Sofia's historic center, Bulgaria, using three established methodologies: RISK-UE, index vulnerability, and SAVE methods. The primary objective is to evaluate the applicability and effectiveness of these methodologies within an Eastern European context, specifically addressing the unique challenges posed by Sofia's historical urban fabric. The city's building stock is characterized by a diverse range of construction typologies, including many

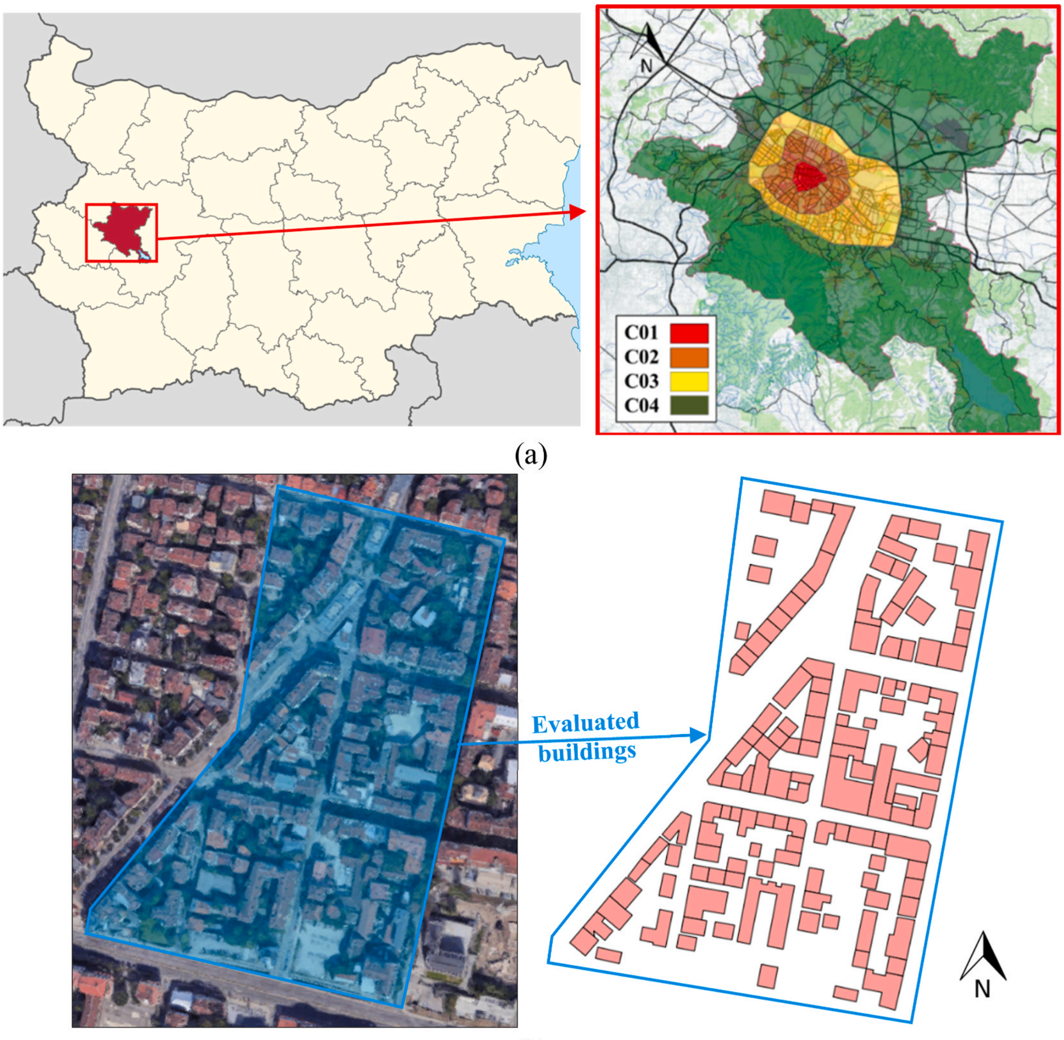

Fig. 1. Case study: municipality of Sofia and subdivision of the sectors (source: commons.wikimedia.org/wiki/Image:Sofia-Capital_in_Bulgaria.svg) (a) and building stock (b).

aggregated structures, which presents a distinct challenge for accurate seismic vulnerability assessments. The choice of methodologies was driven by their established track record and specific strengths in assessing urban seismic risk. RISK-UE has been widely applied in various European cities, offering a robust framework for seismic risk evaluation that allows for comparison across different urban environments. It provides a standardized approach that is well-suited for European contexts, which allows having a valuable benchmark for this study. The vulnerability index methodology was selected for its capability to assess both individual building vulnerabilities and the collective behavior of aggregated structures, which is critical for analyzing Sofia's densely packed urban center. SAVE was chosen for its adaptability to varying levels of data availability, enabling the analysis of areas where detailed building-specific data may be limited or inconsistent.

In applying these methodologies, this research aims to assess their strengths and limitations through a comparative analysis. The study also seeks to validate the methodologies in the context of Eastern European urban centers, contributing to the broader body of research on seismic risk in historically significant areas [14–17,20]. By evaluating these methods in Sofia, a region that has been relatively understudied compared to Western European cities, the research provides new insights into their applicability and reliability in different urban and cultural contexts. Moreover, this study integrates a damage evaluation methodology developed by Lagomarsino and Giovinazzi [4]. This approach allows for a detailed analysis of damage patterns across various building types under different seismic scenarios, thus offering a more comprehensive understanding of potential earthquake damage. The integration of this method enhances the overall assessment, making the results particularly useful for urban planning and risk mitigation strategies.

The manuscript is organized as follows: Section 2 outlines the case study, providing detailed information on the building stock in Sofia's historic center, Section 3 presents the vulnerability assessment methodologies and the results, Section 4 explores the seismic risk scenario analysis, and, finally, Section 5 discusses the findings and offers conclusions.

2. Case study

2.1. Municipality of Sofia and building stock

Sofia, the capital and largest city of Bulgaria, is situated at the foot of Vitosha Mountain in the western part of the country. Centrally located in the Balkans, Sofia is equidistant from the Black Sea and the Adriatic Sea and is closest to the Aegean Sea. The municipality of Sofia is divided into four sectors: C01, historic center, C02, second expansion, C03, third expansion, and C04, periphery, as shown in

Fig. 2. Building typologies of the C01 sector: masonry buildings with steel beam floors with brick infill (a), masonry buildings with reinforced concrete floors (b), reinforcing concrete buildings (c) and disused buildings (d).

Fig. 1a.

The years 1919 and 1945 represent pivotal moments in the historical and architectural evolution of Sofia, shaping the city's urban growth and building practices. These years mark two significant phases of transformation in Sofia's architecture, each shaped by distinct political and socio-economic contexts. After 1919, following the end of World War I, there was a surge in construction, responding to the need for modernization and expansion of the city. This period saw efforts to modernize the urban core, with many masonry structures continuing to dominate, especially in the historic center [21]. The year 1945 marks the end of World War II and a crucial turning point in Bulgaria's political regime. This period is notable for the shift in construction practices, moving towards prefabricated and reinforced concrete buildings under socialist planning, which fundamentally altered Sofia's urban landscape [22]. The reconstruction after the war and the transition to socialism influenced urban planning, emphasizing large-scale housing projects and a departure from the masonry construction that had characterized earlier periods [23]. The bombings of Sofia during World War II and the subsequent need for rebuilding also played a significant role in these shifts, reshaping the city's approach to architecture and planning [24]. As a result, the use of masonry for new constructions declined as the focus shifted towards modernist and socialist urban forms.

The building stock (Fig. 1b) chosen for this investigation is located near the Zhenski Pazar market in the historic center (C01), commonly known as "Ladies Market". This market, the oldest in Sofia, was established shortly after Bulgaria's liberation from Ottoman rule (1908) and has evolved significantly, becoming Sofia's most influential and prestigious trading center in the 20th century. Centrally located between Todor Alexandrov and Slivnitsa boulevards and near the Lion's Bridge, it embodies the historical trade development in downtown Sofia. Three building typologies have been identified in the C01 sector, each differing by construction method: oldest masonry buildings with steel beam floors and brick infill, masonry buildings with reinforced concrete floors, and reinforced concrete buildings.

Masonry buildings with steel beam floors with brick infill are the oldest constructions in the area, constructed either before 1919 or between 1919 and 1945 (Fig. 2a). They are characterized by load-bearing masonry structures with 2–3 floors above ground, primarily for residential use, with the ground floor often used for commercial purposes. These buildings have direct and continuous foundations, steel beam floors with hollow flat blocks, and vertical brick walls 50–60 cm thick. The roofs are typically made of timber, with masonry roofs being rare.

Masonry buildings with reinforced concrete floors were constructed between 1919 and 1970 (Fig. 2b). These buildings also have load-bearing masonry structures but consist of 3–4 floors above ground. The first floor is used for commercial premises, while the upper floors are residential. These buildings have direct and continuous foundations, reinforced concrete floors, cantilevers, and balconies. The vertical structure consists of brick walls 50–60 cm thick, with flat roofs that are usually non-walkable, although timber roofs are rare.

In the end, the reinforced concrete buildings are the most recent, constructed between 1945 and 2010 (Fig. 2c). They have reinforced concrete structures featuring load-bearing reinforced concrete frames, foundations with inverted beams, and vertical structures made of brick blocks. The facades have regular openings and 1.20 m balconies, with typically walkable flat roofs.

All the information was gathered through visual inspections and documentation provided by the Municipality of Sofia. Based on these findings and the diverse range of building typologies, the authors identified this area as particularly interesting for study. The coexistence of both new and old structures, along with the historical significance of the city center, highlights the importance of understanding its seismic vulnerability.

The building stock examined in the study comprises 131 structures: 60 masonry buildings, 63 reinforced concrete buildings, and 8 disused buildings (DB) (Fig. 2d). These DBs have not been included in the seismic vulnerability analysis. The main reason for this exclusion is the extremely poor state of these structures. Many of these disused buildings have severely degraded walls, damaged or missing floors, and are essentially hollow, with no internal components remaining intact. These conditions made it difficult to properly assess their structural integrity.

2.2. Inventory of buildings

2.2.1. The CARTIS form

The buildings have been cataloged by typology, age, number of storeys, floor height, plan area, and volume. This cataloging activity has been conducted by filling out the CARTIS first-level form [25]. This form is aimed at detecting the ordinary building typologies prevalent within municipal or sub-municipal areas, characterized by the homogeneity of the building fabric by the age of first installation or construction and structural techniques. The CARTIS form refers only to ordinary buildings, mainly for homes and services. For this case study, this step was crucial to understand the characteristics of the buildings in the study area of Sofia and to create a database of valuable information to identify the vulnerability index, as shown in the next section.

The CARTIS form was completed based on a field survey conducted by the authors. The survey involved visual inspections of the buildings in the study area in collaboration with local professionals knowledgeable about the region's architectural and structural characteristics. Key information, such as the construction age of the buildings and storey area, was obtained from official records and documents available for the historic district. Other structural details, including the type of construction, floor system, number of stories, and the state of preservation, were gathered through multiple on-site visits. These visits allowed for direct visual inspection of the buildings, ensuring an accurate assessment of their current condition and typology. This comprehensive approach ensured that the data collected for the CARTIS form was both accurate and reflective of the actual conditions of the buildings under study.

The CARTIS form provides the identification and percentage distribution of the most representative building typologies, called MUR 1, MUR 2, MUR 3, and MUR 4 for masonry structures and CAR 1, CAR 2, CAR 3 and CAR 4 for reinforced concrete ones. In our case study, for the old city center of Sofia, two typologies of masonry buildings and one typology of reinforced concrete ones have been considered, respectively associated with acronyms MUR1 (masonry buildings with steel beam floors with brick infill), MUR 2 (masonry buildings with reinforced concrete floors) and CAR1 (reinforced concrete buildings).

According to the CARTIS building classification, 18 % of the buildings are MUR1 typology (M1), 26 % are MUR2 typology (M2), 50 % are CAR1 typology (RC1), and the remaining 6 % are disused buildings (DB) (Fig. 3a). For these buildings, it was observed that 11 % were built before 1919, 22 % between 1919 and 1945, 15 % between 1946 and 1961, 10 % between 1962 and 1971, 18 % between 1972 and 1981, and 18 % were built after 1981 (Fig. 3b). In terms of the number of storeys, 5 % of the buildings have one storey, 18 % have two storeys, 33 % have three storeys, 27 % have four storeys, 11 % have five storeys, 5 % have six storeys, and 2 % have seven storeys (Fig. 3c). Regarding the average surface area, 2 % of the buildings have less than 50 m^2, 17 % have between 50 m^2 and 100 m^2, 47 % have between 100 m^2 and 200 m^2, 21 % have between 200 m^2 and 300 m^2, 8 % have between 300 m^2 and 400 m^2, 2 % have between 400 m^2 and 500 m^2, 1 % have between 600 m^2 and 700 m^2, and 2 % have an average surface area greater than 700 m^2 (Fig. 3d).

2.2.2. *The observed damage assessment*

Numerous studies [26–28] have emphasized the critical role of damage assessment in urban areas with high seismic risk. These studies correlate the structural characteristics of buildings with the extent of damage to develop more precise empirical models for estimating building usability [29]. For this reason, the current state of damage was observed, and the buildings were classified according to the EMS-98 scale [30]. In particular, the EMS-98 scale classifies damage into six grades, ranging from 0 to 5, based on the mean damage grade value derived from a discrete beta distribution. Grade 0 (D0), corresponding to a value of 0, indicates no damage. Grade 1 (D1), with values between 0 and 1, represents negligible to slight damage. Grade 2 (D2), covering values from 1 to 2, indicates moderate damage. Grade 3 (D3), ranging from 2 to 3, corresponds to moderate/substantial damage. Grade 4 (D4), with values spanning from 3 to 4, signifies heavy damage, while Grade 5 (D5), with values between 4 and 5, represents complete collapse.

The observed damage reflects the current condition of the buildings, highlighting any visible structural issues such as cracks, deterioration of balconies, or other damaged elements identified during the field survey. It was found that 25 % of the buildings exhibited no damage (D0), while slight damage (D1) was observed in 30.9 % of the sample. Moderate damage (D2) was present in 17.9 % of the buildings, and 20.3 % showed substantial damage (D3). Lastly, 5.7 % of the buildings were on the verge of collapse (D4) (Fig. 4a).

Based on the observed damage, the predicted state was calculated using the weighted average of damages (μ_D), with the following formula [4,31]:

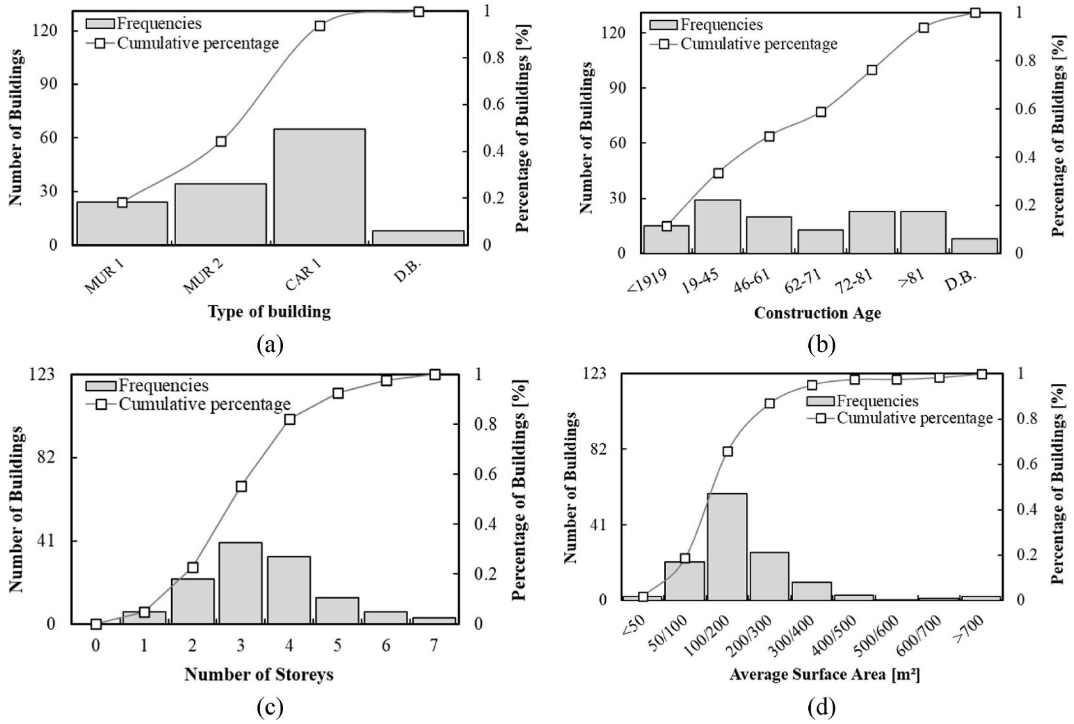

Fig. 3. Building classification: structural typology (a), construction age (b), number of storeys (c), and average surface area (d).

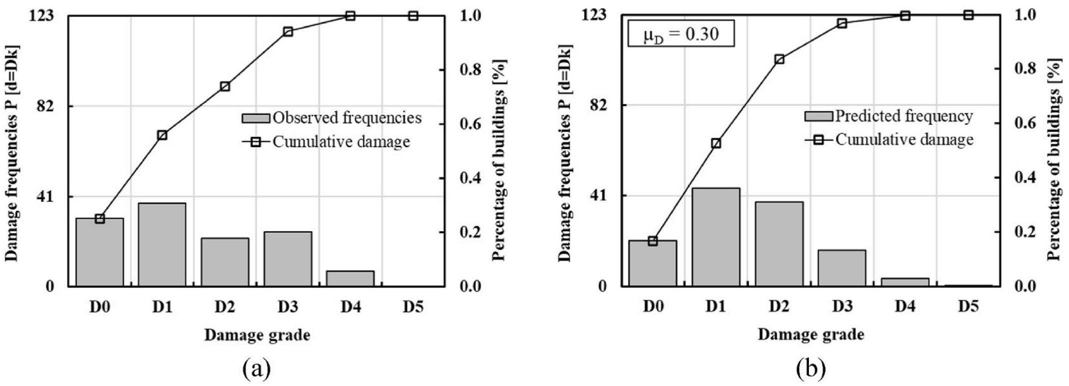

Fig. 4. Observed (a) and predicted (b) damage frequencies.

$$\begin{cases} \mu_D = \sum_{k=1}^{5} p_k k \\ P = \frac{5!}{k!(5-k)!} \cdot \left(\frac{\mu_D}{5}\right)^k \cdot \left(1 - \frac{\mu_D}{5}\right)^{5-k} \end{cases} \tag{1}$$

where k represents the numerical-functional parameter related to the damage level observed, ranging from 0 to 5, as indicated in Ref. [30], and p is the corresponding statistical frequency. The results achieved (Fig. 4b) have shown the predicted frequencies concerning the analyzed urban sector. It is observed that 17 % of the buildings were expected to have no damage (D0), 36 % slight damage (D1), 31 % moderate damage (D2), 13 % substantial damage (D3), and 3 % near collapse (D4). No buildings reached the D5 damage threshold (collapse). So, most of the buildings are expected to sustain minor to moderate damage, with a smaller percentage facing severe damage or near collapse. The absence of buildings reaching the collapse stage (D5) suggests that the overall structural resilience of the area is relatively good.

3. Seismic vulnerability assessment

3.1. Methodologies

3.1.1. RISK-UE

The RISK-UE method [11] implements a typological classification system to categorize structures exhibiting similar seismic behavior. Table 1 presents vulnerability indices for different typologies using the building typology matrix (BTM) proposed by Risk-UE, which aligns closely with the classifications adopted by EMS-98 [30]. Here, V_I^* represents the most probable or plausible value of the vulnerability index (V_I), while V_I^-/ V_I^+ are the bounds of the plausible range of the V_I (usually obtained as 0.5-cut of the membership function), and V_I^{min}/ V_I^{max} are the upper and lower bounds of the possible values of V_I.

Each building type within the studied building stock has been categorized into a specific typological class. In particular, M3.3, identified as composite steel and masonry slabs, has been assigned to the MUR 1 buildings; M3.4, reinforced concrete slabs, has been associated with MUR 2 buildings, and in the end, RC3.1, regularly infilled walls, has been assigned to the CAR 1 buildings. Following this methodology, vulnerability parameters are associated with each typological class.

This new nomenclature associated with the RISK-UE BTM will be used in the following sections.

Subsequentially, they are modified with the so-called behavior modifiers (Table 2), which are used to evaluate a final vulnerability index of each building V_I as follows [11]:

$$V_I = V_I^* + \Delta M_R + \sum_{j=1}^{n} \Delta V_{mj} \tag{2}$$

Table 1
Vulnerability index values for different building typology proposed by Risk-UE.

Typology	Description	Vulnerability indices				
		V_I^{min}	V_I^-	V_I^*	V_I^+	V_I^{max}
M3.3	Composite steel and masonry slabs	0.46	0.527	0.704	0.83	1.02
M3.4	Reinforced concrete slabs	0.30	0.490	0.616	0.793	0.86
RC3.1	Regularly infilled walls	−0.02	0.007	0.402	0.76	0.98

Table 2
Vulnerability index behavior modifiers proposed by Risk-UE.

Behavior modifiers	Masonry Building		Reinforced concrete	
	V_{mj}		ERD level Pre/Low V_{mj}	
Physical conditions	Good	−0.04	Good	0.00
	Bad	0.04	Bad	0.04
N° Storeys above ground	Low (1–2)	−0.08	Low (1–2)	−0.04
	Medium (3–5)	0.00	Medium (3–5)	0.00
	High (6+)	0.08	High (6+)	0.08
Structural system	Wall distance, connections, thickness	−0.04	Irregularity in elevation	0.04
				0.02
		0.04		0
In-plane regularity	Geometry, mass distribution	0.04	In-plane Irregularity	0.04
Irregularity in elevation		0.04	Code Level pre-low	0.16
			medium	0
Roof	Roof weight + Roof Thrust Roof Connections	0.04	high	−0.16
Aggregate building: position	Middle	−0.04	Aggregate buildings (insufficient aseismic joint)	0.04
	Corner	0.04		
	Header	0.06		
Aggregate building: elevation	Staggered floors	0.04	Bow windows	0.04
	Buildings of different height	0.04		
	Buildings with the same height	−0.04		
Foundation	On different levels	0.04	Beams	−0.04
			Connected Beams	0.00
			Isolated Footing	0.04
			Isolated position	0.04

where V_I^* is the most probable or plausible value of the vulnerability index corresponding to the category of the buildings, ΔM_R is a regional modifier which takes into account the peculiarities of the region or building period, while ΔV_{mj} are vulnerability factors or behavior modifiers that incorporate other aspects of the building affecting its seismic behavior.

3.1.2. Vulnerability index

The vulnerability index method [13] is widely employed to identify and characterize the potential seismic weaknesses of a building or group of buildings by assigning a score to each significant structural component. This approach relies on post-seismic damage observations and survey data, assessing numerous elements with an emphasis on the key aspects and features that contribute to building damage. The index vulnerability forms appropriately conceived for masonry and for reinforced concrete are shown in Tables 3 and 4, respectively. For each building, the final vulnerability index is evaluated with the following formula [13]:

$$V_I^* = \sum_{i=1}^{15} S_i \cdot W_i \quad (3)$$

Where S is the class score, and W is the weight. The normalized vulnerability index is subsequentially evaluated as follows:

Table 3
Masonry building vulnerability index form.

Parameters			Class score (S)				Weight (W)
			A	B	C	D	
Isolated	1	Organization of vertical structures	0	0	20	45	1
	2	Nature of vertical structures	0	5	25	45	0.25
	3	Location of the building and foundation type	0	5	25	45	0.75
	4	Distribution of plan-resisting elements	0	5	25	45	1.5
	5	In-plane regularity	0	5	15	45	0.5
	6	Vertical regularity	0	5	25	45	1
	7	Type of floor	0	5	25	45	1
	8	Roofing	0	5	25	45	0.75
	9	Details	0	15	35	45	0.25
	10	Physical conditions	0	5	25	45	1
Aggregate	11	Presence of adjacent buildings with different height	−20	0	15	45	1
	12	Position of the building in the aggregate	−45	−25	−15	0	1.5
	13	Number of staggered floors	0	15	25	45	0.5
	14	Structural or typological heterogeneity among adjacent structural units	−15	−10	0	45	1.2
	15	Percentage difference of opening areas among adjacent facades	−20	0	25	45	1

Table 4
Reinforced concrete building vulnerability index form.

Parameters			Class score (*S*)				Weight (*W*)
			A	B	C	D	
Isolated	1	Type and organization of the resistant system	0	−1	−2		1
	2	Resistant system quality	0	−0.25	−0.5		1
	3	Conventional resistance	0.25	0	−0.25		1
	4	Location of the building and foundation type	0	−0.25	−0.5		1
	5	Type of floor	0	−0.25	−0.5		1
	6	In-plane regularity	0	−0.25	−0.5		1
	7	Vertical regularity	0	−0.5	−1.5		1
	8	Connection and critical elements	0	−0.25	−0.5		1
	9	Elements with low ductility	0	−0.25	−0.5		1
	10	Non-structural elements	0	−0.25	−0.5		1
	11	Physical conditions	0	−0.5	−1	−2.45	1
Aggregate	12	Presence of adjacent buildings with different height	−20	0	15	45	1
	13	Position of the building in the aggregate	−45	−25	−15	0	1.5
	14	Number of staggered floors	0	15	25	45	0.5
	15	Structural or typological heterogeneity among adjacent structural units	−15	−10	0	45	1.2

$$V_{I,M} = \frac{125,5 + V_I^*}{125,5 + 526,5} \tag{4}$$

$$V_{I,RC} = \frac{105,5 + V_I^*}{105,5 + 504,8} \tag{5}$$

3.1.3. SAVE project

The SAVE procedure (Updated Tools for the Seismic Vulnerability Evaluation of the Italian Real Estate and Urban Systems) aims to reduce the inherent uncertainty in the EMS-98 vulnerability classification [8]. This is achieved by identifying typological features that serve as vulnerability modifiers and assigning each a numerical weight, calibrated using an extensive database of seismic damage from significant earthquakes in Italy, starting with the 1980 Irpinia earthquake up to the present. The database, compiled from post-earthquake survey forms, includes information on approximately 170,000 buildings across about 500 municipalities. The majority of surveyed buildings were masonry structures, and most data fields in the database pertain to this type of construction. Consequently, the survey forms lack specific data on vulnerable elements of reinforced concrete structures, such as short columns. Therefore, correlations regarding the vulnerability of reinforced concrete buildings are derived from the limited available data.

The SAVE method starts with the association of the *SPD* based on the vertical structural typology (Table 5). In particular, B, identified as regular masonry, has been assigned to the M3.3 buildings; C_m, mixed reinforced concrete and masonry, has been associated with M3.4 buildings, and in the end, D, reinforced concrete, has been assigned to the RC3.1 buildings. As highlighted by the previous methodologies, understanding only the vertical structure of a building may be insufficient for accurately determining its vulnerability class. The seismic performance of a building can vary significantly due to numerous factors that can either enhance or impair its behavior during seismic events. So, the *SPD* of a single building is evaluated as follows [8]:

$$SPD = SPD_{VS} + \sum_{i=1}^{n} PS_i \cdot SPD_{VS} \tag{6}$$

where SPD_{VS} is the *SPD* associated with the vertical structure typology, while PS_i are the modifier parameters. The PS_i are parameters associated with different building characteristics, such as the floor type, presence of isolated columns in masonry buildings, presence of tie roads, pre-existent damage, building location in the block, infill panel regularity (only for r.c. buildings), site topography, etc. [8]. Since these parameters are not always fully available, the SAVE procedure can independently assess the influence of each parameter when determining the vulnerability class. This allows the procedure to be applied regardless of the number of known parameters. In Table 6, the parameters considered for this study are shown.

Table 5
SAVE SPD building classification according to the typology of vertical structure.

Category		Typology of the vertical structure	SPD_{VS}
B		Stones, regular masonry, mixed (r.c.+ masonry on different floors), hollow bricks	1.87
C	C_1	Solid bricks	1.64
	C_m	Mixed (r.c.+ masonry, both on all the floors)	1.51
D		Frame, reinforced concrete or steel	1.29

Table 6
SAVE PS_i parameters considered for this study.

	PS_1			PS_2		PS_3		PS_4				PS_5	
	Floor type			Pushing Roof		Horizontal connections		Position of the building in the aggregate				Regularity in elevation	
	Deformable	Rigid	Semi rigid	No	Yes	0	1	Corner	Out	Middle	Isolated	No	Yes
A	0.332	−0.133	−0.085	−0.054	0.054	0.063	−0.063	0.084	0.074	−0.017	−0.001	–	–
B	0.221	−0.104	−0.14	−0.065	0.065	0.074	−0.074	0.065	0.056	−0.008	0.059	–	–
Cm	0.172	−0.167	−0.07	−0.058	0.058	0.039	−0.039	0.046	0.035	0.006	0.019	–	–
C1	0.173	−0.135	−0.168	−0.030	0.030	0.091	−0.091	0.046	0.053	0.008	0.037	–	–
D	–	–	–	–	–	–	–	−0.001	0.004	−0.03	0.037	0.103	−0.103

3.2. Results and comparison

The results have been evaluated in terms of vulnerability index (V_I), a parameter conventionally defined to range from 0 to 1 [4,32]. V_I numerical values are purely conventional scores used to quantify the behavior of buildings, providing a standardized measure of a building's vulnerability to earthquakes [32]. For the sake of simplicity, a 0–1 range has been chosen, with values close to 1 for those of the most vulnerable buildings and values close to 0 for the ones representative of the structures conformed to the recent standard codes. Specifically, a low vulnerability level is associated with values from 0 to 0.2, medium-low from 0.2 to 0.4, medium from 0.4 to 0.6, medium-high from 0.6 to 0.8, and high from 0.8 to 1.

Based on the RISK-UE methodology, equation (2) yields values of V_I ranging from −0.02 to 1.2. Min-max normalization was applied to standardize these values between 0 and 1. For the vulnerability index, the final value is already normalized according to equations (4) and (5). Regarding the SAVE methodology, a correlation between *SPD* and V_I has been established. In this correlation, a SPD of less than 1.1 indicates a low vulnerability level. SPD values between 1.1 and 1.4 correspond to a medium-low vulnerability level, values between 1.4 and 1.7 indicate a medium vulnerability level, values from 1.7 to 2 denote a medium-high vulnerability level, and values above 2 signify a high vulnerability level.

The results are summarized in Table 7 and Fig. 5, which present the percentage of buildings associated with each seismic vulnerability level as determined by the respective vulnerability index methodologies. Specifically, Table 7 details the percentages for each vulnerability assessment method across different building typologies, while Fig. 5 illustrates the overall distribution of these percentages across all the typological classes.

In the RISK-UE methodology, for the typological class RC3.1, 44 % of the buildings present a low seismic vulnerability, while the remaining 56 % present a medium-low seismic vulnerability. For the typological class M3.3, 4 % of the buildings have a medium-low seismic vulnerability, 79 % have a medium seismic vulnerability, and 17 % have a medium-high seismic vulnerability. In the typological class M3.4, 8 % of the buildings exhibit low seismic vulnerability, 86 % exhibit medium-low seismic vulnerability, and 6 % exhibit medium seismic vulnerability. Across all typological classes, 25 % of the buildings have low seismic vulnerability, 55 % have medium-low seismic vulnerability, 17 % have medium seismic vulnerability, and 3 % have medium-high seismic vulnerability.

For the vulnerability index methodology, it was observed that for typological class RC3.1, 16 % of the buildings have low seismic vulnerability, 67 % have medium-low seismic vulnerability, and 17 % have medium seismic vulnerability. For typological class M3.3, 79 % of the buildings exhibit medium seismic vulnerability, while 21 % exhibit medium-high seismic vulnerability. In the typological class M3.4, 44 % of the buildings have medium-low seismic vulnerability, and 56 % have medium seismic vulnerability. Across all typological classes, 8 % of the buildings exhibit low seismic vulnerability, 47 % exhibit medium-low seismic vulnerability, 41 % exhibit medium seismic vulnerability, and 4 % exhibit medium-high seismic vulnerability.

Using the SAVE project methodology, it was found that for typological class RC3.1, 2 % of the buildings exhibit low seismic vulnerability and 98 % exhibit medium-low seismic vulnerability. For typological class M3.3, 42 % of the buildings have medium seismic vulnerability, and 58 % have medium-high seismic vulnerability. In the typological class M3.4, 72 % of the buildings present medium-low seismic vulnerability and 28 % present medium seismic vulnerability. Across all typological classes, 1 % of the buildings have low seismic vulnerability, 72 % have medium-low seismic vulnerability, 16 % have medium seismic vulnerability, and 11 % have medium-high seismic vulnerability.

Using the QGIS open-source tool [33], the vulnerability of the analyzed building stock has been visually represented (Fig. 6). QGIS is a Geographic Information System developed in C++ with a graphical user interface (GUI). This tool enables the processing of building plan layouts, acquired in a CAD environment and accurately georeferenced using the WGS84 (World Geodetic System, 1984) coordinate system into a mathematical model. A unique feature of the software is its ability to automatically recognize and convert the generated shapefile lines of constructions (vector formats for representing geometric identities) into polygons.

Different results have been obtained from the three methodologies. The RISK-UE methodology indicated the highest percentage for the low seismic vulnerability class. The SAVE methodology showed the highest percentages for the medium-low and medium-high seismic vulnerability classes. The vulnerability index methodology demonstrated the highest percentage for the medium seismic vulnerability class. On average, the seismic vulnerability index for each building typology is comparable (Fig. 7). Specifically, the RC3.1 building typology falls into the medium-low seismic vulnerability class. The M3.4 building typology falls into the medium-low to medium seismic vulnerability class, while the M3.3 building typology exhibits the highest values, corresponding to medium to medium-high seismic vulnerability.

These differences among the three methodologies arise from their distinct frameworks and data use. The SAVE methodology yielded higher vulnerability values, influenced by its focus on Italian building typologies and the limited use of only five out of twelve

Table 7
Percentage of buildings at each seismic vulnerability level by vulnerability assessment methodology and building typology.

Seismic vulnerability	RISK-UE			Vulnerability Index			SAVE		
[–]	RC3.1	M3.4	M3.3	RC3.1	M3.4	M3.3	RC3.1	M3.4	M3.3
Low	44 %	8 %	–	16 %	–	–	2 %	–	–
Medium-Low	56 %	86 %	4 %	67 %	44 %	–	98 %	72 %	–
Medium	–	6 %	79 %	17 %	56 %	79 %	–	28 %	42 %
Medium-High	–	–	17 %	–	–	21 %	–	–	58 %
High	–	–	–	–	–	–	–	–	–

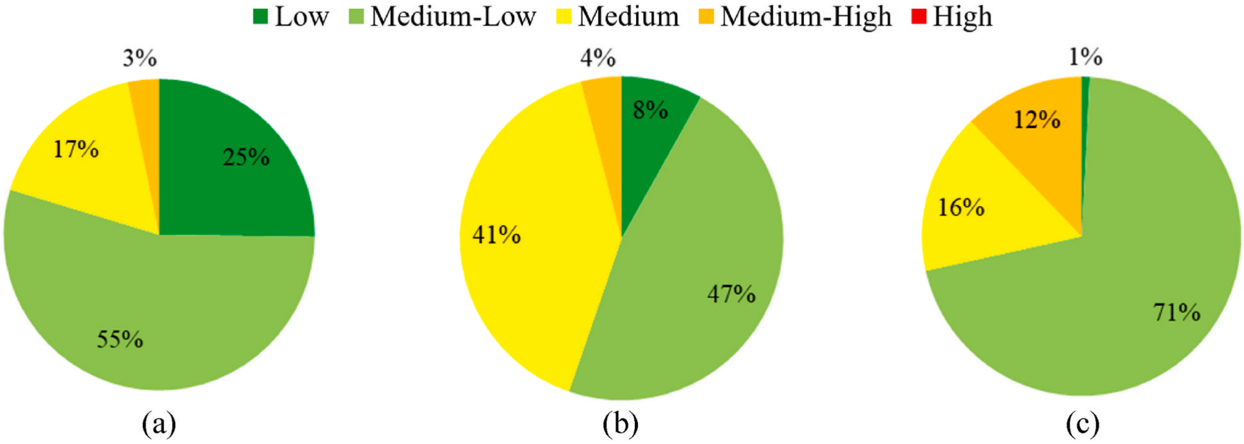

Fig. 5. Percentage of buildings at each seismic vulnerability level: RISK-UE (a); Vulnerability index methodology (b); SAVE (c).

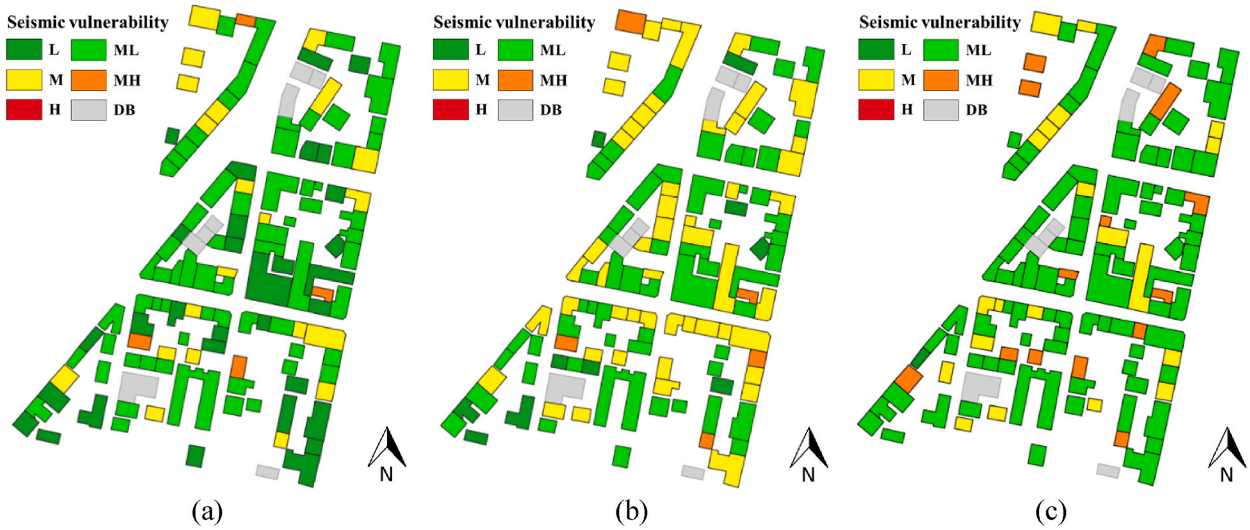

Fig. 6. Seismic vulnerabilities distribution within the building stock, obtained with the Risk-UE (a), vulnerability index (b) and SAVE (c) methodologies.

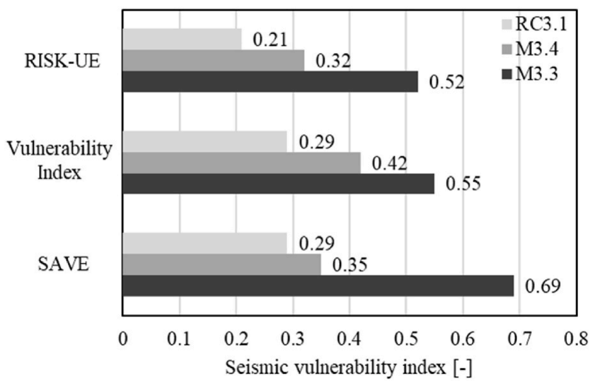

Fig. 7. Comparison of the average seismic vulnerability index for building typology.

available parameters. In contrast, the RISK-UE and vulnerability index methodologies produced comparable results, though the latter considers more detailed aggregated building data. This distinction led to consistently higher and more conservative vulnerability estimates from the vulnerability index method.

For the risk scenario analysis presented in the following section, the Vulnerability Index Methodology was chosen for several important reasons. Primarily, this method enables a more thorough analysis of the building stock by integrating detailed structural information, which is essential for evaluating the diverse and complex building typologies found in the historic center. Unlike the SAVE method, the Vulnerability Index Method provides a broader evaluation, effectively capturing the diversity of building types. Additionally, compared to the RISK-UE method, it considers more detailed information regarding the aggregate state of structures. The vulnerability indices derived through this method were consistently higher than those from the RISK-UE method, offering a more conservative estimate. This conservatism introduces an additional safety margin into the risk scenario analysis, helping to ensure that the vulnerability of buildings is not underestimated. Given the critical importance of accurately assessing seismic vulnerability in

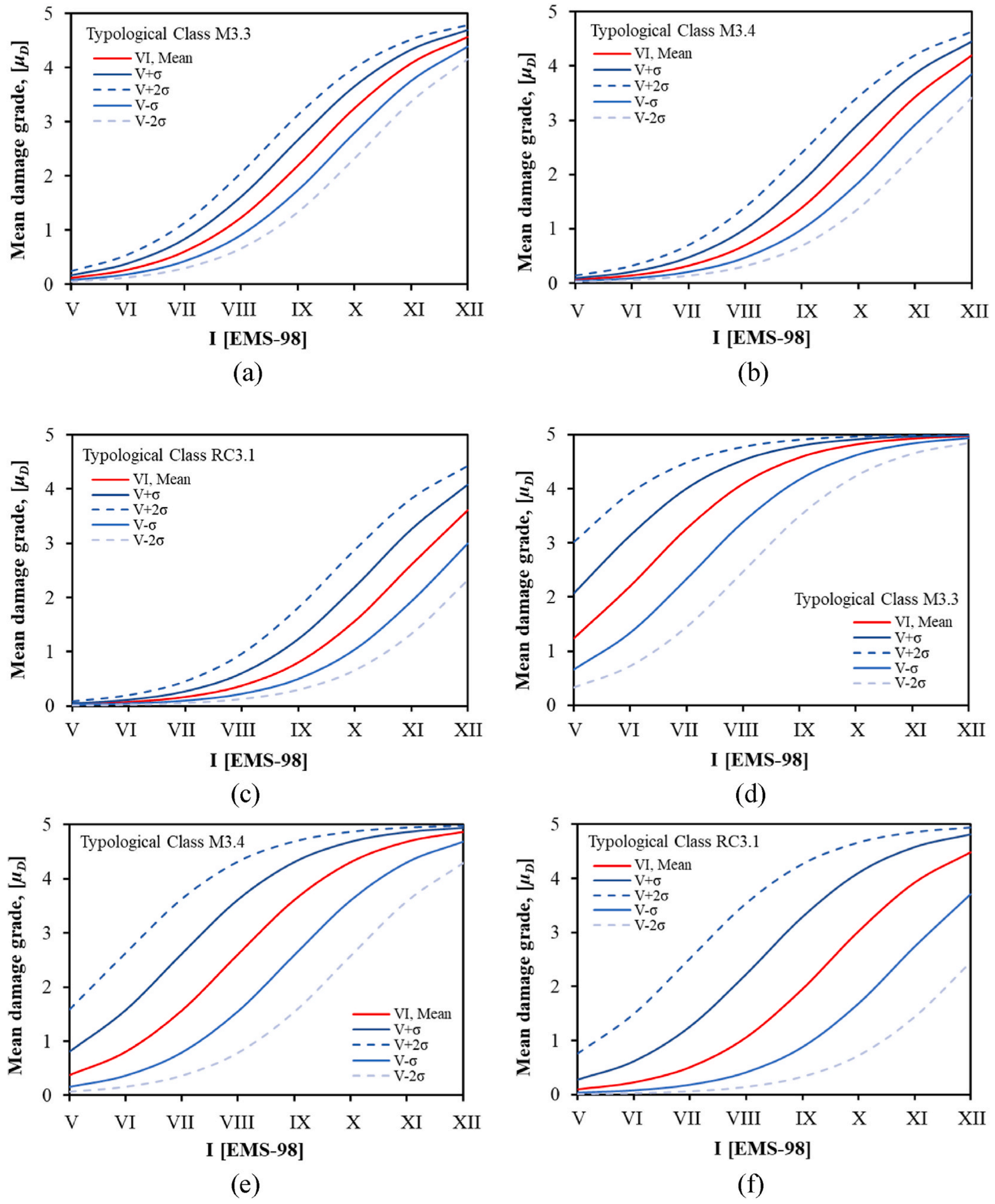

Fig. 8. I(EMS-98)-μ_D vulnerability curves: Lagomarsino et al. (a-b-c) and calibrated (d-e-f).

historic urban environments, this approach was deemed the most appropriate for the study.

4. Risk scenario analysis

4.1. Sofia seismic history

Historical documents confirm the occurrence of destructive earthquakes in the Sofia area between the 15th and 18th centuries. Before the 19th century, Sofia was a small town within the Ottoman Empire, resulting in limited earthquake reports. In the 19th century, Sofia experienced two significant earthquakes: the 1818 earthquake, with an epicentral intensity (I_0) of VIII-IX MSK, and the 1858 earthquake, with an I_0 of IX-X MSK (recently confirmed to be the same in terms of EMS-98) [34]. The 1858 earthquake caused heavy destruction in the town of Sofia and the appearance of thermal springs in the western part of the town [34]. In the 20th century, the most significant earthquake near Sofia was the 1917 event, with a magnitude (M_w) of 5.3 (I_0 = VII-VIII MSK), which caused considerable damage to Sofia and nearby villages. No earthquakes with a magnitude of 5 or higher have occurred in the Sofia seismic zone since 1917. The most notable recent event was a 4.3 M_w earthquake in 1980, located about 30 km from Sofia in the northern part of the Sofia seismic zone.

Drawing on Sofia's seismic history, the 1858 earthquake was selected for the macroseismic intensity scenario. The estimated M_w for this event ranges from 6.0 to 6.5, so a value of 6.3 M_w was used. The maximum macroseismic intensity (I_0) was set to IX (EMS-98), in accordance with references [34,35].

4.2. Mean damage grade

Once the vulnerability indices are obtained and the macroseismic intensity range is evaluated, the mean damage grade, μ_D, can be calculated using the I(EMS-98)-μ_D vulnerability curves. These curves are essential, as they provide a direct relationship between seismic intensity and expected damage levels, enabling a more accurate estimation of potential damage patterns and their likelihood, which is crucial for risk assessment and preparedness planning. Using μ_D, it is possible to generate various damage distribution histograms for different intensities and vulnerability index values through a probabilistic approach.

For the implementation, the following analytical expression proposed by Lagomarsino et al. [4] to correlate the hazard (*I*) with the mean damage grade value has been considered:

$$\mu_D = 2,5 \cdot \left[1 + \tanh\left(\frac{I + 6.25 \cdot V_I - 13.1}{Q}\right)\right] \tag{7}$$

where seismic hazard *I* is expressed in terms of macroseismic intensity, V_I is the vulnerability index of the building, and Q is the ductility index, which is equal to 2.3 [4]. The results for each building typological class are presented in Fig. 8a-b-c. The curves were derived from the mean vulnerability index values, calculated as the average of the vulnerability indices for each building typology.

According to the mean curves obtained for the building typological class RC3.1, at a macroseismic intensity of V, the damage grade is 0.11, indicating no damage (D0). At the maximum macroseismic intensity of IX, the damage grade is 2.19, indicating moderate damage (D2). For the typological class M3.3, at a macroseismic intensity of V, the damage grade is 0.05, indicating no damage (D0). At the maximum macroseismic intensity of IX, the damage grade is 1.39, indicating slight damage (D1). For the typological class M3.4, at a macroseismic intensity of V, the damage grade is 0.05, indicating no damage (D0). At the maximum macroseismic intensity of IX, the damage grade is 1.39, indicating slight damage (D1).

As it is possible to see, the results of Lagomarsino et al.'s formula are not conservative because they are too low. In fact, with the maximum intensity of this zone, IX (EMS-98), the maximum damage is moderate/substantial damage (D3). This does not align with the expected outcomes based on Sofia's seismic history. According to the previous section, for the maximum macroseismic intensity of IX, significant damage is anticipated, particularly for a large portion of buildings, especially those made of masonry. This happened because Lagomarsino et al.'s formula is calibrated on different building typologies. So, the formula has been properly calibrated based on Sofia's seismic history as follows:

$$\mu_D = 2,5 \cdot \left[1 + \tanh\left(\frac{I + \Psi \cdot V_I - 13.1}{Q}\right)\right] \tag{8}$$

where *I* is always the seismic hazard expressed in terms of macroseismic intensity, Ψ is a factor assumed equal to 12.50, and it is related to the variation of the slope of the curve, and Q is the ductility factor, which always assumed a value of 2.3.

Using the new formula, reasonable results (Fig. 8d and e-f) have been obtained. In particular, according to the main curves, it was observed that for the typological class RC3.1, at a macroseismic intensity of V, the damage grade is 0.09, indicating no damage (D0). At the maximum macroseismic intensity of IX, the damage grade is 1.95, indicating moderate damage (D2). For the typological class M3.3, at a macroseismic intensity of V, the damage grade is 1.25, indicating moderate damage (D2). At the maximum macroseismic intensity of IX, the damage grade is 4.57, indicating collapse (D5). For the typological class M3.4, at a macroseismic intensity of V, the damage grade is 0.37, indicating moderate damage (D2). At the maximum macroseismic intensity of IX, the damage grade is 3.61, indicating heavy damage (D4).

4.3. Damage scenarios

4.3.1. Damage model prediction

The concept of risk pertains to the economic, social, and environmental impacts caused by a natural event in a specific area. This research is based on predictive analysis, evaluating potential scenarios by disaggregating the hazard using various source models. Consequently, hazard disaggregation procedures illustrate the combination of magnitude, M_w, and epicenter distance, R, in determining the expected occurrence probability of a specific seismic event in a given region [36].

For this purpose, four seismic events with varying magnitudes (M_w 4.0, 5.0, 6.0, and 7.0) were chosen based on Sofia's seismic history. Consequently, different damage scenarios were examined, considering the maximum seismic effects for epicenter distances ranging from 5 km to 20 km. For the evaluation of the seismic intensities, two attenuation laws for the ground shaking have been considered:

$$I = \frac{3}{2} \cdot (M_w - 1) \tag{9}$$

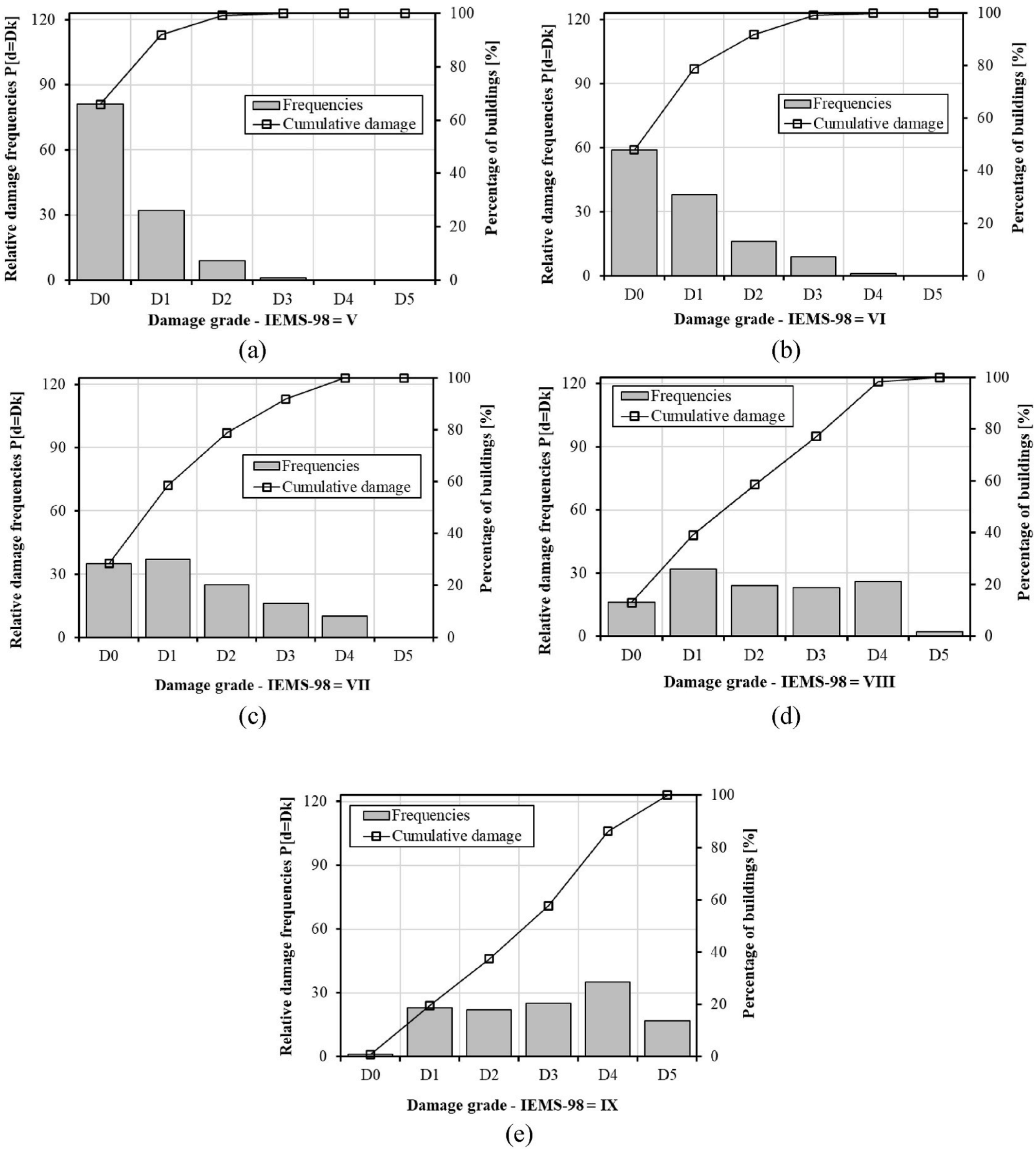

Fig. 9. Damage probability matrix for V (a), VI (b), VII (c), VII (d), IX (e) macroseismic intensities (IEMS-98).

$$I = I_0 - 3 \cdot log\left(\frac{r}{h}\right) - 1,3 \cdot 0,002 \cdot (R - h) \tag{10}$$

The first attenuation law [37] is a function only of the magnitude M_w. Instead, the second one [38] is a function of M_w, I_0, the epicentral distance R, and the depth h. The latter has been fixed at a depth of 10 km. This value was chosen based on the depth distribution analysis conducted in Ref. [38], which indicates that the majority of earthquakes in Bulgaria are primarily concentrated in the upper crust.

So, considering the four magnitudes and four epicenter distances, 5 km, 10 km, 15 km, and 20 km, different levels of macroseismic intensities have been obtained. They have been classified in the EMS-98 intensities scale. With the first attenuation law, intensities ranging from V to IX have been obtained. Instead, with the second one, seven different intensities ranging from III to IX have been obtained.

Referring to the mean damage grade μ_D, seven damage scenarios have been simulated. The damage distribution has been defined employing the Damage Probability Matrix (DPM) depicted in Fig. 9. It is important to note that only the results for intensities ranging from V to IX are presented, as macroseismic intensities below grade V did not induce any effects on the structures, resulting in no damage to any of the buildings. The results are presented as a QGIS plot in Fig. 10.

Based on the findings, for lower intensities (V), the majority of the buildings remain undamaged, with over 65 % showing no structural damage (D0), suggesting that the buildings in the studied area are generally well-prepared for low to moderate seismic events. However, even at this intensity, a notable proportion (approximately 26 %) already exhibits slight damage (D1), indicating that certain types of structures are less resilient, even under relatively low seismic stress. As the intensity increases to VI, the percentage of undamaged buildings decreases significantly (to 48 %), while both slight and moderate damage categories (D1 and D2) increase

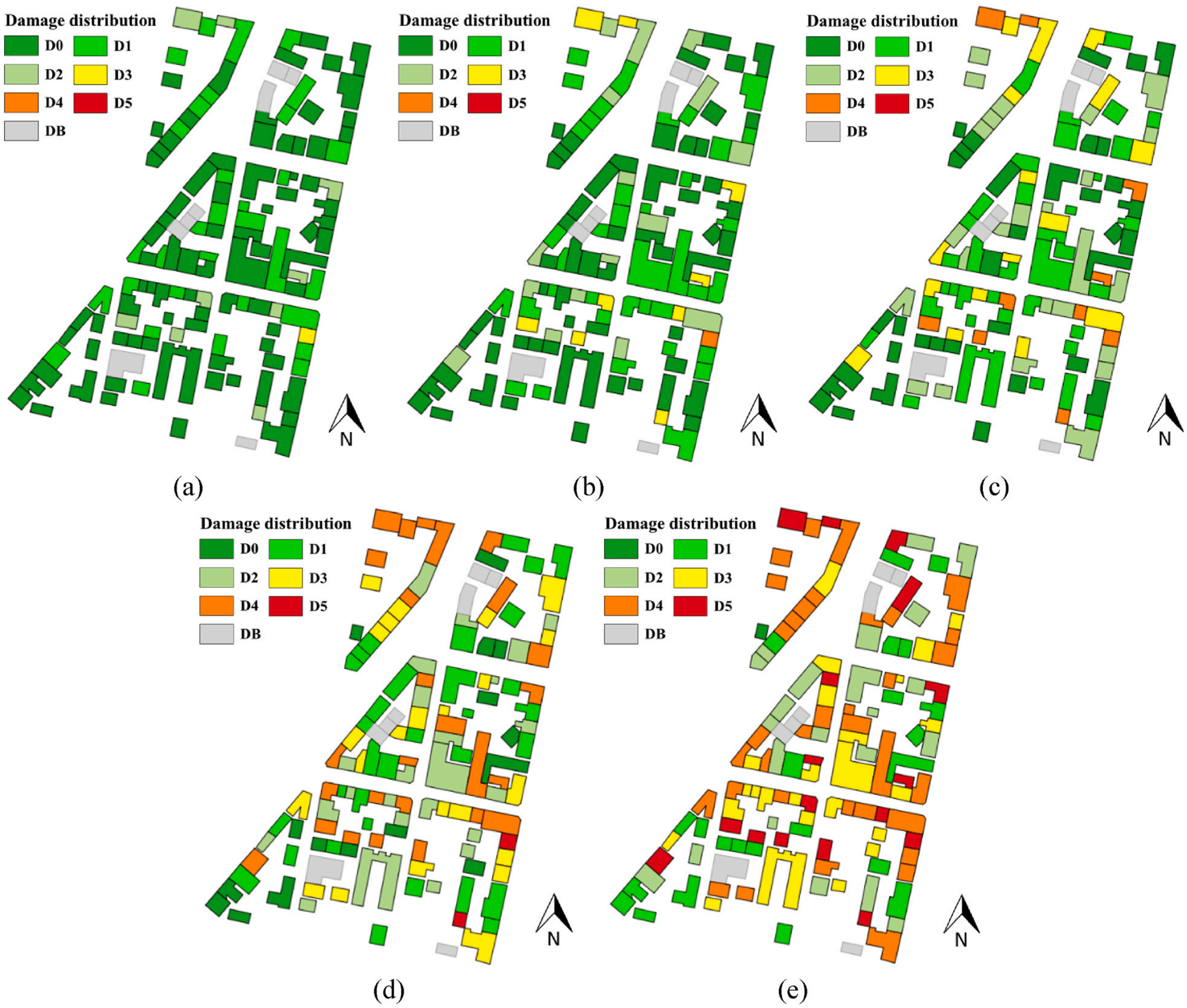

Fig. 10. Simulated damage scenarios for the building stock of Sofia: V (a), VI (b), VII (c), VII (d), IX (e) macroseismic intensities (IEMS-98).

noticeably. This suggests that at this level, a substantial number of buildings are not only showing signs of distress but also transitioning into moderate damage, where structural elements might begin to be compromised. At intensities of VII and above, the structural integrity of many buildings begins to deteriorate more rapidly. The proportion of buildings suffering moderate to substantial damage (D2 and D3) climbs steadily, and by intensity VIII, a concerning 18.7 % of buildings are substantially damaged, with 8.1 % nearing collapse (D4). This indicates a clear escalation in the vulnerability of the built environment as the intensity grows, with the potential for severe safety risks in urban areas. At maximum intensity IX, the data highlights a critical shift, where nearly 30 % of the buildings are on the brink of collapse (D4), and 13.8 % have completely collapsed (D5). This finding emphasizes the extreme fragility of the building stock under such seismic conditions, where a substantial portion of the infrastructure becomes unsafe.

4.4. Prediction of collapsed and unusable buildings loss estimation

Estimating functional loss, defined as the proportion of unusable and collapsed buildings, is crucial for urban planning and retrofit strategies as it informs effective structural repair measures and ensures life safety. The model used is based on the likelihood of exceeding specific damage levels. According to Ref. [39], the equations for unusable and collapsed buildings are as follows:

$$P_{unusable} = P[D_3] \cdot W_{ei,3} + P[D_4] \cdot W_{ei,4} \tag{11}$$

$$P_{collapse} = P[D_5] \tag{12}$$

here $P[D_i]$ represents the probability of reaching a particular damage grade (ranging from D_1 to D_5), and $W_{ei,j}$ are multiplier factors that denote the percentage of buildings considered unusable. According to Ref. [17], the multiplier factors have been considered equal to 0.4 and 0.6 for $W_{ei,3}$ and $W_{ei,4}$, respectively. Results are shown in Fig. 11.

For typology RC3.1, the probability of becoming unusable remains relatively low, with only a 1 % chance at intensity VII and gradually increasing to 17 % by intensity IX. The most notable observation here is the absence of collapse risk at any intensity level, indicating that this building type is relatively robust in terms of structural integrity, even under high seismic stress. The gradual increase in unusability suggests that while RC3.1 buildings may endure moderate to severe damage, they are generally well-constructed to avoid catastrophic failure. This implies that retrofitting efforts, if needed, could focus on preventing functionality loss rather than addressing collapse risks, making RC3.1 buildings a stable choice for seismic regions.

In contrast, typology M3.3 exhibits much higher vulnerability. The probability of buildings becoming unusable rises significantly with seismic intensity, from 2 % at intensity V to a peak of 50 % at intensity VIII, before decreasing to 20 % at intensity IX. This drop at intensity IX could be indicative of the fact that many buildings either collapsed or have already become unusable by this stage. The sharp increase in the probability of collapse, from 8 % at intensity VIII to 67 % at intensity IX, further demonstrates the fragility of M3.3 structures under extreme seismic conditions. This typology is highly susceptible to severe damage and eventual collapse, suggesting that it would require substantial reinforcement or reconstruction to withstand high-intensity earthquakes. These findings indicate that M3.3 is the most vulnerable of the typologies, with a pressing need for preventive measures to avoid large-scale collapses during intense seismic events.

Typology M3.4 shows a more moderate vulnerability pattern compared to M3.3. The probability of buildings becoming unusable rises gradually, reaching 44 % at intensity IX, and the collapse probability at this intensity is relatively low at 3 %. However, the steady increase in unusability, especially as intensities VIII and IX are reached, suggests that this typology, while less prone to total collapse, still faces significant risks of being rendered unusable. The moderate collapse probability indicates that while M3.4 buildings are somewhat more resilient than M3.3, they still require attention to prevent severe structural damage under high seismic stress.

5. Conclusions

This paper presented a study of seismic vulnerability assessment of building stock in the city center of Sofia, Bulgaria. In particular, a comparative study of three seismic vulnerability assessment methods, namely the RISK-UE, the index vulnerability, and the SAVE, was proposed.

The initial phase of the study focused on creating a building database encompassing 123 buildings. Data collection was conducted using the CARTIS form, which gathered essential information such as structural typology, number of storeys, age, and other relevant details required for the seismic vulnerability assessment. This information was obtained through visual inspections and documentation provided by the Municipality of Sofia. Following data collection, the seismic vulnerability index of the buildings was assessed using three different methods.

The results indicate that all three methodologies yielded similar average vulnerability index values across the three identified building classes within the building stock. In particular, the three approaches showed that the most vulnerable building class is the masonry M3.3 type, masonry buildings with steel beam floors with brick infill, with a medium vulnerability, while the less vulnerable buildings are the reinforced concrete ones of RC3.1 type, with a medium-low vulnerability. For the third building class of M3.4 type, masonry buildings with reinforced concrete floors, a medium-low vulnerability has been found.

The SAVE methodology indicated higher vulnerability values. This outcome is attributed to the methodology being designed for Italian building typologies, relying on experiences specific to that context. Additionally, the limited availability of building information contributed to this result, as only five out of the twelve available parameters were considered in the assessment. In contrast, the RISK-UE and vulnerability index methodologies produced similar results. However, the RISK-UE methodology does not take into

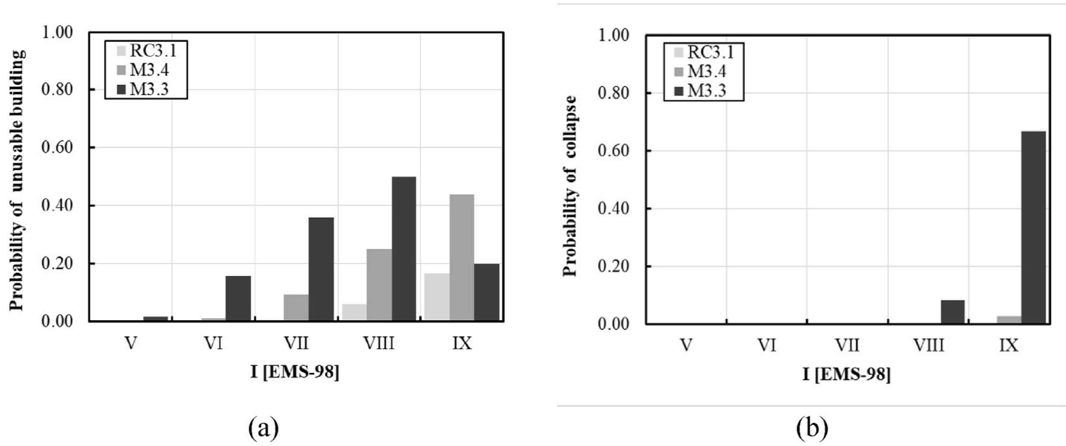

Fig. 11. Prediction of unusable (a) and collapsed (b) buildings.

account much information about the aggregate state of the buildings as the vulnerability index method does. As a result, the vulnerability index method appeared to be the most accurate among the three approaches used. Additionally, the vulnerability indices obtained through this method were consistently higher than those derived from the RISK-UE method, providing a more conservative estimate. This conservatism introduces an extra safety margin into the risk scenario analysis, helping to ensure that the vulnerability of buildings is not underestimated. Given the crucial importance of accurately assessing seismic vulnerability in historic urban environments, this approach was considered the most suitable for this study.

In the context of risk scenario analysis, the damage grade μ_D was determined for various macroseismic intensities according to Sofia's seismic history. At lower intensities, the data suggests a general resilience among buildings, though certain structures show signs of weakness even under mild seismic conditions. As seismic intensity increases, a clear trend emerges: the number of buildings experiencing damage rises, signaling a transition from minor issues to more severe structural distress. This progression indicates that many buildings, while initially withstanding minor seismic events, struggle to maintain integrity as the forces intensify. When examining specific building typologies, the differences in their responses to seismic stress become apparent. Typology RC3.1 demonstrates a notably high level of structural integrity, even as intensities increase, with damage primarily resulting in usability issues rather than structural collapse. This suggests that interventions for such buildings could prioritize maintaining functionality over major structural reinforcements. Typology M3.4 shows a moderate pattern of vulnerability, with a steady rise in damage but a lower likelihood of catastrophic failure. This highlights the need for targeted measures to reduce damage and maintain usability without necessarily focusing on collapse prevention. In contrast, typology M3.3 is markedly more vulnerable, with a sharp increase in damage severity as seismic intensity rises. The high susceptibility of this typology to severe damage, including the risk of collapse, indicates a pressing need for substantial reinforcement to ensure safety during stronger seismic events.

In conclusion, this study provided a comprehensive seismic vulnerability assessment of Sofia's city center, offering valuable insights for both future research and immediate policy implementation. The findings lay a strong foundation for future studies to refine seismic vulnerability assessments, not only in Sofia, but also in other urban areas with similar characteristics. The methodology can be adapted for seismic risk analysis in other cities, contributing to a broader understanding of urban seismic vulnerability. Practically, the study offers critical information for urban planners and emergency responders, aiding in the development of more effective risk mitigation strategies. Pinpointing the most at-risk building typologies enables prioritization of reinforcement efforts, especially for structures in densely populated or strategically important areas. Additionally, the insights gained support the formulation of emergency response plans, such as the optimal placement of evacuation routes and safe zones based on the distribution of vulnerable buildings, ultimately enhancing both preparedness and resilience in urban settings.

CRediT authorship contribution statement

Gaetano Pianese: Writing – review & editing, Data curation, Writing – original draft, Software, Investigation, Formal analysis. **Nicola Chieffo:** Writing – review & editing, Software, Investigation, Formal analysis, Data curation. **Gabriele Milani:** Writing – review & editing, Supervision, Methodology. **Doncho Partov:** Writing – review & editing, Supervision, Data curation, Conceptualization. **Antonio Formisano:** Writing – review & editing, Validation, Supervision, Resources, Project administration, Methodology, Data curation, Conceptualization.

Declaration of competing interest

The authors declare that they have no known competing financial interests or personal relationships that could have appeared to influence the work reported in this paper.

Data availability

Data will be made available on request.

References

[1] G. Nicodemo, M. Pittore, A. Masi, V. Manfredi, Modelling exposure and vulnerability from post-earthquake survey data with risk-oriented taxonomies: AeDES form, GEM taxonomy and EMS-98 typologies, Int. J. Disaster Risk Reduc. 50 (2020), https://doi.org/10.1016/j.ijdrr.2020.101894.
[2] R. Nascimbene, Investigation of seismic damage to existing buildings by using remotely observed images, Eng. Fail. Anal. 161 (2024) 108282, https://doi.org/10.1016/j.engfailanal.2024.108282.
[3] H. Crowley, R. Pinho, J.J. Bommer, A probabilistic displacement-based vulnerability assessment procedure for earthquake loss estimation, Bull. Earthq. Eng. 2 (2004), https://doi.org/10.1007/s10518-004-2290-8.
[4] S. Lagomarsino, S. Giovinazzi, Macroseismic and mechanical models for the vulnerability and damage assessment of current buildings, Bull. Earthq. Eng. 4 (2006), https://doi.org/10.1007/s10518-006-9024-z.
[5] M.M. Kassem, Nazri F. Mohamed, E.N. Farsangi, B. Ozturk, Development of a uniform seismic vulnerability index framework for reinforced concrete building typology, J. Build. Eng. 47 (2022), https://doi.org/10.1016/j.jobe.2021.103838.
[6] M.M. Kassem, F.M. Nazri, E.N. Farsangi, B. Ozturk, Improved vulnerability index methodology to quantify seismic risk and loss assessment in reinforced concrete buildings, J. Earthq. Eng. 26 (2022), https://doi.org/10.1080/13632469.2021.1911888.
[7] D. Benedetti, V. Petrini, On the seismic vulnerability of masonry buildings: an evaluation method (in Italian), L'industria Delle Costruzioni 149 (1984) 66–74.
[8] G. Zuccaro, F. Cacace, Seismic vulnerability assessment based on typological characteristics. The first level procedure "SAVE.", Soil Dynam. Earthq. Eng. 69 (2015) https://doi.org/10.1016/j.soildyn.2014.11.003.
[9] G. Zuccaro, V. Albanese, F. Cacace, C. Mercuri, F. Papa, A.G. Pizza, et al., Seismic vulnerability evaluations within the structural and functional survey activities of the COM bases in Italy, AIP Conf. Proc. 1020 (2008), https://doi.org/10.1063/1.2963797.
[10] N. Lantada, J. Irizarry, A.H. Barbat, X. Goula, A. Roca, T. Susagna, et al., Seismic hazard and risk scenarios for Barcelona, Spain, using the Risk-UE vulnerability index method, Bull. Earthq. Eng. 8 (2010), https://doi.org/10.1007/s10518-009-9148-z.
[11] Z. Milutinovic, G. Trendafiloski, Risk-UE an advanced approach to earthquake risk scenarios with applications to different european towns. Report to WP4: Vulnerability of Current Buildings, 2003.
[12] M. Shakya, GNDT II level approach for seismic vulnerability assessment of Unreinforced Masonry (URM) building stock, Journal of Science and Engineering 3 (2015), https://doi.org/10.3126/jsce.v3i0.22384.
[13] A. Formisano, G. Florio, R. Landolfo, F.M. Mazzolani, Numerical calibration of an easy method for seismic behaviour assessment on large scale of masonry building aggregates, Adv. Eng. Software 80 (2015), https://doi.org/10.1016/j.advengsoft.2014.09.013.
[14] N. Chieffo, F. Clementi, A. Formisano, S. Lenci, Comparative fragility methods for seismic assessment of masonry buildings located in Muccia (Italy), J. Build. Eng. 25 (2019), https://doi.org/10.1016/j.jobe.2019.100813.
[15] M. Mosoarca, I. Onescu, E. Onescu, B. Azap, N. Chieffo, M. Szitar-Sirbu, Seismic vulnerability assessment for the historical areas of the Timisoara city, Romania, Eng. Fail. Anal. 101 (2019), https://doi.org/10.1016/j.engfailanal.2019.03.013.
[16] T.M. Ferreira, R. Vicente, J.A.R. Mendes da Silva, H. Varum, A. Costa, Seismic vulnerability assessment of historical urban centres: case study of the old city centre in Seixal, Portugal, Bull. Earthq. Eng. 11 (2013), https://doi.org/10.1007/s10518-013-9447-2.
[17] N. Chieffo, M. Mosoarca, A. Formisano, I. Apostol, Seismic vulnerability assessment and loss estimation of an urban district of Timisoara, IOP Conf. Ser. Mater. Sci. Eng. 471 (2019), https://doi.org/10.1088/1757-899X/471/10/102070.
[18] G. Cocco, A. D'Aloisio, E. Spacone, G. Brando, Seismic vulnerability of buildings in historic centers: from the "urban" to the "aggregate" scale, Front Built Environ 5 (2019), https://doi.org/10.3389/fbuil.2019.00078.
[19] N. Chieffo, A. Formisano, R. Landolfo, G. Milani, A vulnerability index based-approach for the historical centre of the city of Latronico (Potenza, Southern Italy), Eng. Fail. Anal. 136 (2022), https://doi.org/10.1016/j.engfailanal.2022.106207.
[20] P. Lamego, P.B. Lourenço, M.L. Sousa, R. Marques, Seismic vulnerability and risk analysis of the old building stock at urban scale: application to a neighbourhood in Lisbon, Bull. Earthq. Eng. 15 (2017), https://doi.org/10.1007/s10518-016-0072-8.
[21] S. Hirt, K. Stanilov, The perils of post-socialist transformation: residential development in Sofia, in: K. Stanilov (Ed.), The Post-Socialist City: Urban Form and Space Transformations in Central and Eastern Europe after Socialism, Springer Netherlands, Dordrecht, 2007, pp. 215–244, https://doi.org/10.1007/978-1-4020-6053-3_11.
[22] E. Stanoeva, Ideology and urbanism in a flux, SE. Eur. 41 (2017), https://doi.org/10.1163/18763332-04102002.
[23] S. Hirt, Landscapes of postmodernity: changes in the built fabric of Belgrade and Sofia since the end of socialism, Urban Geogr. 29 (2008), https://doi.org/10.2747/0272-3638.29.8.785.
[24] I. Gigova, The city and the nation: Sofia's trajectory from glory to rubble in WWII, J. Urban Hist. 37 (2011), https://doi.org/10.1177/0096144210391612.
[25] G. Zuccaro, M. Dolce, F.L. Perelli, D. De Gregorio, E. Speranza, CARTIS: a method for the typological-structural characterization of Italian ordinary buildings in urban areas, Front Built Environ 9 (2023), https://doi.org/10.3389/fbuil.2023.1129176.
[26] M. Zucconi, R. Ferlito, L. Sorrentino, Validation and extension of a statistical usability model for unreinforced masonry buildings with different ground motion intensity measures, Bull. Earthq. Eng. 18 (2020), https://doi.org/10.1007/s10518-019-00669-2.
[27] R. Sisti, M. Di Ludovico, A. Borri, A. Prota, Damage assessment and the effectiveness of prevention: the response of ordinary unreinforced masonry buildings in Norcia during the Central Italy 2016–2017 seismic sequence, Bull. Earthq. Eng. 17 (2019), https://doi.org/10.1007/s10518-018-0448-z.
[28] A. Rosti, M. Rota, A. Penna, Damage classification and derivation of damage probability matrices from L'Aquila (2009) post-earthquake survey data, Bull. Earthq. Eng. 16 (2018), https://doi.org/10.1007/s10518-018-0352-6.
[29] M. Biglari, A. Formisano, A. Davino, Seismic vulnerability assessment and fragility analysis of Iranian historical mosques in Kermanshah city, J. Build. Eng. 45 (2022), https://doi.org/10.1016/j.jobe.2021.103673.
[30] G. Grünthal, European Macroseismic Scale 1998, vol. 15, 1998.
[31] N. Chieffo, A. Formisano, The influence of geo-hazard effects on the physical vulnerability assessment of the built heritage: an application in a district of Naples, Buildings 9 (2019), https://doi.org/10.3390/buildings9010026.
[32] S. Giovinazzi, S. Lagomarsino, A macroseismic method for the vulnerability assessment of buildings. 13th World Conference on Earthquake Engineering, 2004.
[33] QGIS Development Team, QGIS Geographic Information System, Open Source Geospatial Foundation Project, 2014. http://qgis.osgeo.org. Qgisorg.
[34] D. Solakov, I. Aleksandrova, I. Popova, G. Georgieva, S. Simeonova, Earthquake scenarios for the cities of Sofia, rousse and vratsa. Information & security, Int. J. 24 (2009), https://doi.org/10.11610/isij.2406.
[35] G. Solomos, A. Pinto Vieira, S. Dimova, A Review of the Seismic Hazard Zonation in National Building Codes in the Context of Eurocode 8, OPOCE, 2008.
[36] S. Barani, D. Spallarossa, P. Bazzurro, Disaggregation of probabilistic ground-motion Hazard in Italy, Bull. Seismol. Soc. Am. 99 (2009), https://doi.org/10.1785/0120080348.
[37] M.I. Todorovska, I. Paskaleva, R. Glavcheva, M.I. Todorovska, I. Paskaleva, R. Glavcheva, Earthquake source parameters for seismic hazard assessment: examples in Bulgaria. 10th European Conference on Earthquake Engineering, 1995.
[38] S.D. Simeonova, D.E. Solakov, G. Leydecker, H. Busche, T. Schmitt, D. Kaiser, Probabilistic seismic hazard map for Bulgaria as a basis for a new building code, Natural Hazards and Earth System Science 6 (2006), https://doi.org/10.5194/nhess-6-881-2006.
[39] R. Vicente, S. Parodi, S. Lagomarsino, H. Varum, J.A.R.M. Silva, Seismic vulnerability and risk assessment: case study of the historic city centre of Coimbra, Portugal, Bull. Earthq. Eng. 9 (2011), https://doi.org/10.1007/s10518-010-9233-3.